The Effect of Heat Flux on the Fire and Chemical Properties of Oak Wood (*Quercus petraea*)

Martin Zachar [a,*] Alena Párničanová [b] Danica Kačíková [c] Iveta Čabalová [d] and Lucia Zacharová [e]

Selected fire properties of oak wood (mass loss, burning rate, and charring rate) and its chemical composition (extraction substances, lignin, cellulose, hemicellulose) were assessed. Oak wood samples with dimensions of 50 × 40 × 50 mm (l × w × t) were thermally loaded by a heat flux of 15, 20, 25, and 30 kW·m^{-2}, using a ceramic infrared heater with a power of 1000 W. At the given thermal loading, the mass loss ranged from 26% to 47%, whereas the burning rate ranged from 0.0365 to 0.0584%·s^{-1}. The maximum thickness of charred layer was 20 mm, and the charring rate reached values from 0.65 to 0.87 mm·min^{-1}, in a time interval of 1800 s. With increasing thermal loading, the content of extraction substances increased by 30% and the content of lignin increased slightly as well. In contrast, the content of hemicelluloses decreased by 10.3%. This indicates that hemicelluloses are the least thermally resistant wood component. The obtained results can be used as basic data for future testing using medium-sized tests. Subsequently, they can be compared with the input parameters for calculating the fire resistance of wooden constructions elements, which will be the subject of further research.

DOI: 10.15376/biores.20.1.860-876

Keywords: Oak wood; Mass loss; Burning rate; Charring rate; Chemical composition

Contact information: a: Assoc. Prof. Martin Zachar, Technical University in Zvolen, Faculty of Wood Sciences and Technology, Department of Fire Protection, T. G. Masaryka 24, 960 01 Zvolen, Slovakia; b: Ing. Alena Párničanová, Technical University in Zvolen, Faculty of Wood Sciences and Technology, Department of Fire Protection, T. G. Masaryka 24, 960 01 Zvolen, Slovakia; c: Prof. Danica Kačíková, Technical University in Zvolen, Faculty of Wood Sciences and Technology, Department of Fire Protection, T. G. Masaryka 24, 960 01 Zvolen, Slovakia; d: Assoc. Prof. Iveta Čabalová, Technical University in Zvolen, Faculty of Wood Sciences and Technology, Department of Chemistry and Chemical Technologies, T. G. Masaryka 24, 960 01 Zvolen, Slovakia; Dr. Lucia Zacharová, National Forest Centre, Forest Research Institute, T. G. Masaryka 22, 960 01 Zvolen, Slovakia;
**Corresponding authors: zachar@tuzvo.sk*

INTRODUCTION

Wood is used as a construction material because it is affordable and in the case of prefabricated houses it enables time saving in construction (Hrovatin 2005). It is important to ensure the strength and longevity of buildings, as well as to pay attention to their fire resistance (Zanatta *et al.* 2018). During fires in buildings made with structural elements of type D2 and D3, wood usually represents the main fuel. An important part of ensuring the fire safety of buildings is the knowledge of fire dynamics, which is an important starting point, for example, in the design of buildings, controlled evacuation, as well as in the process of determining the fire causes (Kačíková *et al.* 2017).

Wood is composed of polymers that are susceptible to thermal loading and is subject to destruction, while the thermal oxidation reactions take place in it, where the degradation reagent is *e.g.* flame or a radiant heat source acting on a sample (Reinprecht 1997; Zanatta *et al.* 2018). The content of polymers, lignin, cellulose, and hemicelluloses in the structure of wooden fibres has an impact on the properties of wood structure during thermal degradation (Salmen *et al.* 2011).

Lignin is the most thermally stable component of wood. It decomposes at temperatures above 250 to 500 °C. During degradation, charring takes place; therefore, it is subsequently difficult to ignite it (Osvald 2010; Poletto *et al.* 2015). Decomposition of cellulose takes place at temperatures of 276 to 350 °C. Hemicelluloses are the most thermally unstable, such that they decompose at temperatures of 180 °C (Lowden and Hull 2013; Poletto *et al.* 2015). In the fast pyrolysis of individual wood components using a single particle reactor, the results show different rates of decomposition of wood components. Decomposition of hemicelluloses has been found to be faster compared to lignin and cellulose (Mensah *et al.* 2023).

Charring occurs in the process of pyrolysis, which takes place at high temperatures and constant pressures in an oxygen-free environment for the thermal decomposition of wood as an organic material (Richter *et al.* 2019; Kravetz *et al.* 2020; Qin *et al.* 2021). During this process, Carbon monoxide and soot are produced (Hasburgh and Dietenberger 2001; Liu *et al.* 2016). The charring temperature is approximately 300 °C, at which a charred layer of wood is formed (Booth 1987; White and Nordheim 1992; Chen *et al.* 2016; Findorák *et al.* 2016).

The charring rate is influenced by wood density and its moisture, external heat flux, and oxygen concentration in the ambient air, as well as by the type of wood and the burning direction (Njankouo *et al.* 2004; Mikkola 2007; Cachim and Franssen 2008; Salmen *et al.* 2011). According to STN EN 1995-1-2 (Eurocode 5), it is important to know the value of the charring rate, which enters into the calculation of the fire resistance of wooden constructions. The charring rate is determined based on the charring depth and the time of exposure to thermal loading (Martinka *et al.* 2018). In addition, it is important to investigate the fire causes, which is in line with NFPA 921 (2021). In accordance with NFPA 921 (2017), the charring rate of wood under laboratory conditions and exposure to a heat source from one side is determined from 0.17 to 4.23 $mm \cdot min^{-1}$. In line with EN 1995-1-2 2, the proposed charring rate of solid and glued laminated softwood and beech is constant, approximately 0.6 $mm \cdot min^{-1}$, and it decreases with increasing density (Friquin 2011). The value of the charring rate of grown/solid and glued laminated hardwood and beech with a bulk density greater than 450 $kg \cdot m^{-3}$ is 0.50 $mm \cdot min^{-1}$ (Špilák 2018). The experiments showed that the charring rate is not constant. At the beginning of burning, the charring rate is usually faster than the rate after the formation of the charred layer, because the charred layer acts as an increasing thermal insulation between the exposed surface and the pyrolyzed wood, which results in degression of the charring rate during the first phase of combustion. Once the first few millimetres of charring are formed, the rate is stable (Friquin 2011).

In practice, the charred layer is used as a retardation treatment. It absorbs thermal radiation well; however, it is a poor conductor of heat because of its porous structure (Bartlett *et al.* 2019). When evaluating the spread of fire, the depth of charred layer is analysed according to a technical standard (Eurocode 5). To determine burning time and fire intensity, the charring depth is defined as the distance between the outer surface of the original element and the position of the line between the charred layer and the rest of the

cross-section (Zhou *et al.* 2020). According to other authors, the charred layer is the boundary between non-degraded wood and charred wood (Kim *et al.* 2020). Thermally degraded wood has a thinned cell wall (Salmen *et al.* 2011). In the case of wooden constructions, it is important to identify the residual cross-section, which is able to withstand the load during fire; therefore, it is necessary to know the thickness of charring (Kamenická *et al.* 2018). In line with Babrauskas (2005), the load-bearing capacity of wooden beams and columns decreases after flashover. The charred layer shows good heat-insulating properties and at the same time prevents the air to enter the internal parts of the cross-section, which slows down the burning (Babrauskas 2005).

Fire properties, *i.e.*, mass loss, burning rate, thickness of charred layer, and charring rate, serve as basic input data as computer-supported modelling of indoor fires. The data on the burning rate and the charring rate are also used in calculations of the fire safety of buildings, especially in case of load-bearing constructions made of structural elements of type D3.

In terms of fire safety, it is important to know the content of individual chemical components of wood, *i.e.*, hemicellulose, cellulose, lignin, and extractive substances because their degradation causes the loss of mechanical properties of wood, which can lead to disruption of stability of wooden constructions.

The aim of the paper was to assess selected fire characteristics of oak wood (mass loss, burning rate, and charring rate) and its chemical composition (content of extractive substances, lignin, cellulose and hemicelluloses) after thermal loading carried out using a measuring apparatus described in the Utility Model No. 9373 registered by the Industrial Property Office of the Slovak Republic.

EXPERIMENTAL

Materials

Test samples were prepared from the log of sessile oak (*Quercus petraea*) harvested during winter in the location of Kremenný Jarok (Linaj) 320 m.a.s.l., stand number 607, managed by the University Forest Enterprise. The trunk was 110 years old. The air-dried samples were sawn in tangential direction to dimensions of 50 × 40 × 50 mm (l × w × t). Subsequently, the selected samples without anatomical defects were sorted into 4 groups with 10 samples in each group (for loading with a heat flux of 15, 20, 25 and 30 $kW \cdot m^{-2}$). The samples were then dried in a drying oven and adjusted to a moisture content of 10 +/- 0.15%. The density of test samples was 681 ± 0.03 $kg \cdot m^{-3}$. Elemental analysis of oak wood was carried out as follows: carbon (C, 507 g/kg) was determined according to ISO 10694, nitrogen (N, 1.65 g/kg) according to ISO 13878, and sulphur (S, 236 mg/kg) according to ISO 15178, using elemental analysis with thermal decomposition. Phosphor (P, 0.162 g/kg), calcium (Ca, 0.452 g/kg), magnesium (Mg, 0.048 g/kg), and potassium (K, 0.373 g/kg) was determined according to ISO 11885, using atomic emission spectrometry with inductively coupled plasma.

Thermal loading was carried out using a measuring apparatus described in the Utility Model No. 9373 registered by the Industrial Property Office of the Slovak Republic. The apparatus (Fig. 1) consisted of a ceramic infrared heater (with power of 1 000 W, Ceramicx Ltd., Gortnagrough, Ireland), accurate digital scales (Radwag PS 3500.R2, RADWAG Balances and Scales, Radom, Poland), control device (METREL HSN0203, Metrel d.d. Horjul, Slovenia), temperature measuring devices (Data logger

ALMEMO® 710, Ahlborn Mess und Regelungstechnik GmbH, Holzkirchen, Germany), type "K" thermocouples with a thickness of 0.5 mm (Omega Engineering Inc., Norwalk, CT, USA), and an initiation burner (propane burner CLASIC CZ, Ltd., Řevnice, Czech Republic).

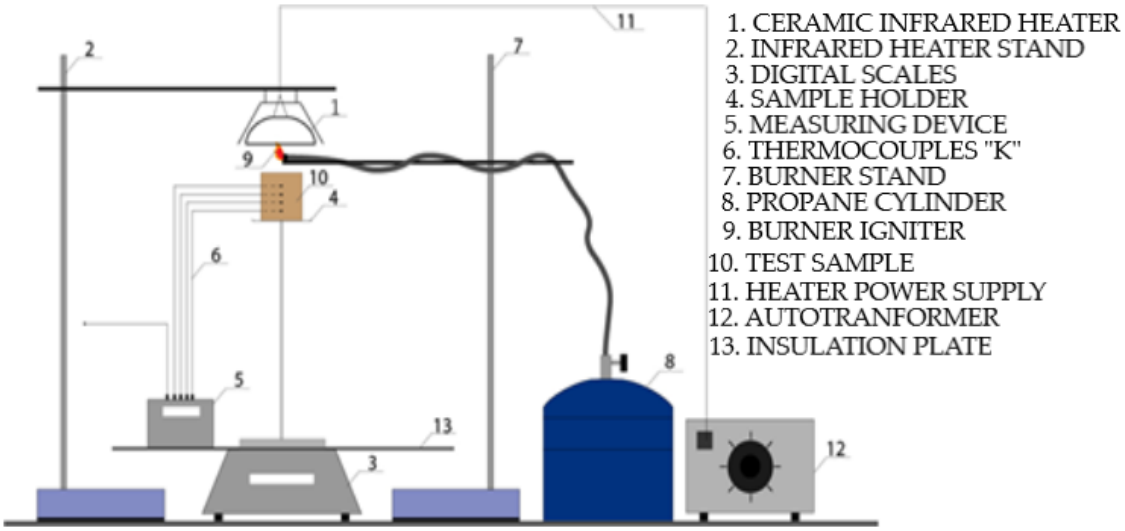

Fig. 1. Scheme of laboratory apparatus

Individual thermocouples were inserted into the test samples in a distance of 10 mm (T1), 20 mm (T2), 30 mm (T3), and 40 mm (T4) from the thermally loaded surface.

Mass Loss

The weight of each sample was recorded at 5 seconds intervals for 1800 seconds using laboratory scales. Based on the measured values, the mass loss δ (τ) (%) was subsequently determined using Eq. 1,

$$\delta(\tau) = \frac{\Delta m}{m(\tau_0)} \cdot 100 = \frac{m(\tau_0) - m(\tau)}{m(\tau_0)} \cdot 100 \quad (1)$$

where $\delta(\tau)$ is the mass loss over time (τ) (%), $m(\tau 0)$ is the original mass of the sample (g), $m(\tau)$ is the mass of the sample over time (τ) (g), and Δm is the mass difference (g).

Burning Rate

The burning rate was determined according to Eq. 2,

$$\vartheta = \frac{\delta(\tau) - \delta(\tau + \Delta\tau)}{\Delta\tau} \quad (2)$$

where v is the burning rate (%·s^{-1}), $\delta(\tau)$ is the mass loss over time (τ) (%), $\delta(\tau + \Delta\tau)$ is the mass loss over time ($\tau + \Delta\tau$) (%), and $\Delta\tau$ is the time interval in which mass values are recorded (s).

Charring Rate

The charring rate was calculated according to Eq. 3,

$$\beta = \frac{d\ char}{t} \quad (3)$$

where β is the charring rate (mm·min^{-1}), d_{char} is the charring thickness (mm), and t is the time of thermal loading (min).

Chemical Composition of Wood

The rest of the samples (after removing the charred layer) after the thermal loading with a heat flux of 15, 20, 25, and 30 kW·m^{-2} and reference sample were disintegrated into sawdust, and fractions from 0.5 mm to 1.0 mm in size were used for the chemical analyses. The extractives content (EXT) was extracted for 8 h with six siphonings per hour, using a Soxhlet apparatus with a mixture of absolute ethanol (Merck, Germany) and toluene specified for analysis, according to the ASTM D1107-21 (2021). The holocellulose (HOLO) content was determined to the method by Wise *et al*. (1946), cellulose (CEL) according to Seifert (1956), and lignin (LIG) according to Sluiter *et al*. (2012). Hemicelluloses (HEMI) were calculated as the difference between the holocellulose and the cellulose content. Measurements were carried out on four replicates per sample. The results were presented as oven-dry wood percentages.

RESULTS AND DISCUSSION

Selected fire properties of oak wood samples, *i.e.*, the mass loss and the charring thickness, were measured using the measuring apparatus (described above), and subsequently, the burning rate and the charring rate were calculated according to Eqs. 2 and 3 (see Experimental Section). Chemical composition was determined according to ASTM D 1107-21.

Mass Loss of Samples

The mass loss of oak wood samples depending on the thermal loading with a heat flux of 15, 20, 25, and 30 kW·m^{-2} had an increasing tendency, and it increased with increasing thermal loading of samples (Fig. 2).

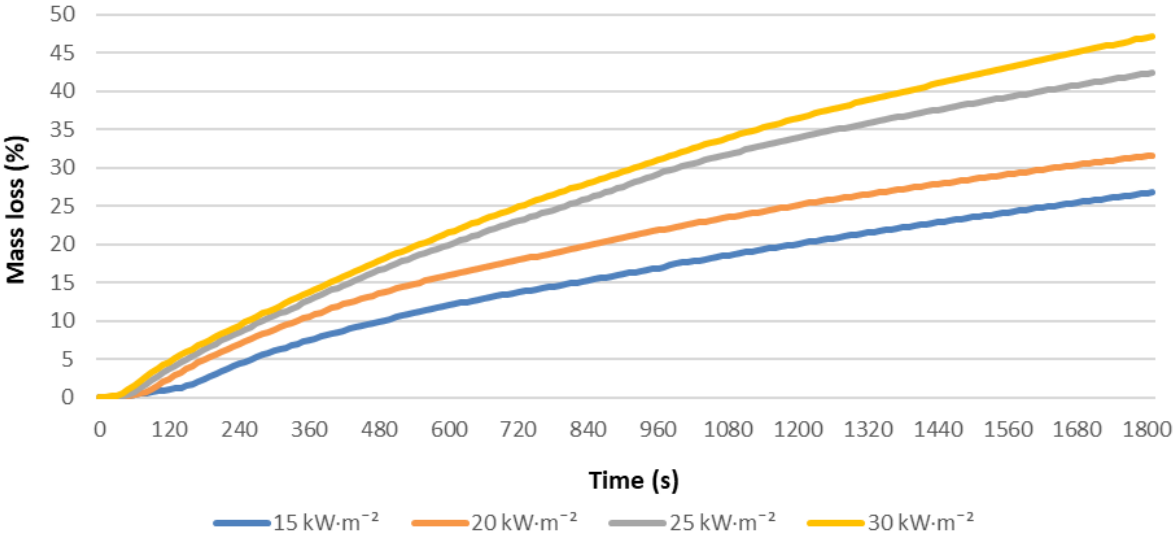

Fig. 2. Mass loss of samples over time with varying heat fluxes

At a heat flux of 15 kW·m^{-2}, the mass loss was 26%. At increased heat flux of 20 kW·m^{-2}, the mass loss was 32%. At a heat flux of 25 kW·m^{-2}, the mass loss increased to 41%. The sample loaded by a heat flux of 30 kW·m^{-2} reached the greatest mass loss, *i.e.*, almost 47%. With increasing heat flux from 15 to 30 kW·m^{-2}, there was an increase in mass loss in the range from 26 to 47%.

The achieved results are also confirmed by previous measurements carried out by other authors who used samples of similar dimensions, and approximately the same source of thermal loading. Protić *et al.* (2020) determined the mass loss of oak wood loaded by a heat flux of 30 kW·m^{-2} using a mass loss calorimeter, which is a device used for reaction-to-fire characterization of a solid sample in a similar way as in a cone calorimeter. The material testing procedure was set up in ISO 17554 and ISO 13927. Kmeťová *et al.* (2022) determined the mass loss of oak wood samples with dimensions of 10 × 40 × 50 mm to 86 % of its original weight. The samples were loaded by a ceramic heater with a power of 1000 W, in a distance of 40 mm from the thermally loaded surface, during a loading time of 600 seconds.

Burning Rate

The values of the burning rate of oak wood samples depending on thermal loading with a heat flux of 15, 20, 25, and 30 kW·m^{-2} had an upward tendency. With increasing thermal loading, the burning rate also increased (Fig. 3). Based on the variation in the burning rate curves of the oak wood samples, the samples reached the maximum burning rate in a shorter time, with increasing heat flux.

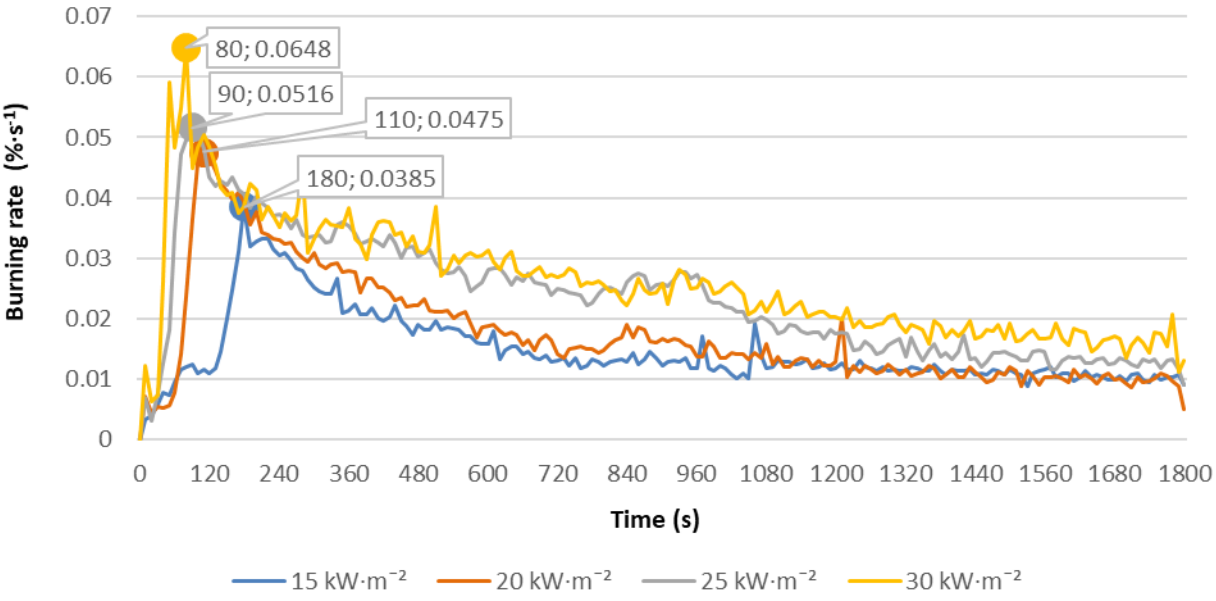

Fig. 3. Burning rate of thermally loaded samples over time with varying heat fluxes

At a heat flux of 15 kW·m^{-2}, the maximum burning rate of 0.0358%·s^{-1} was reached in 180 seconds. At a heat flux of 20 kW·m^{-2}, the maximum burning rate was 0.0475%·s^{-1}, which was reached in 110 seconds. At a heat flux of 25 kW·m^{-2}, the maximum burning rate was 0.0516%·s^{-1}, which was reached in 90 seconds. The sample loaded by a heat flux of 30 kW·m^{-2} reached the maximum burning rate of 0,0648%·s^{-1} in 80th seconds from the

beginning of thermal loading. The results confirmed that the time to reach the maximum burning rate varied significantly depending on the heat flux. With increasing heat flux, the maximum burning rate increased and time interval to reach the burning rate decreased.

According to the results of Zachar *et al.* (2021), for Norway spruce samples dried to absolute humidity at constant weight, loaded with a heat flux of 15 kW·m^{-2} the maximum burning rate was 0.09%·s^{-1}; at a higher heat flux of 30 kW·m^{-2}, the maximum burning rate was 0.32 %·s^{-1}. Kačíková and Makovická-Osvaldová (2009) determined the burning rate of individual parts of a tree – wood from the log, branches, and roots, using samples with dimensions of 10 × 12 × 150 mm prepared from Scots pine, white fir, European larch, and Norway spruce. The samples were thermally loaded by a ceramic infrared heater with a power of 1000 W for 180 seconds. The lowest average burning rate (0.033 %·s^{-1}) was determined for spruce roots, and the maximum average burning rate (0.090 %·s^{-1}) was determined for spruce log. The authors stated that the burning rate depends on the type of wood as well as the part of the three from which the wood is cut. According to their experiments, the lowest burning rate of pine, fir, spruce, and larch was measured for wood from branches, their values ranged from 0.033 to 0.039 %·s^{-1}.

Temperature Profile

The temperature profile in the sample under thermal loading depends on the magnitude of heat flux. The higher heat flux is acting on the sample, the earlier it reaches the charring temperature (300 °C). At heat fluxes of 15, 20, and 25 kW·m^{-2} acting on the sample of oak wood, charring occurred only to a depth of 10 mm from the thermally loaded surface, on thermocouple T1. At a heat flux of 15 kW·m^{-2}, a temperature of 300.4 °C was reached on thermocouple T1 in a time of 1030 s; at a heat flux of 20 kW·m^{-2}, a temperature of 300.6 °C was reached in a time of 820 s; at a heat flux of 25 kW·m^{-2}, a temperature of 300.7 °C was reached in a time of 750 s; and at a heat flux of 30 kW·m^{-2}, a temperature of 300.2 °C was reached in a time of 620 s. The temperature progression in the samples under a thermal loading of 15, 20, 25 and 30 kW·m^{-2} are shown in Figs. 4, 5, 6 and 7.

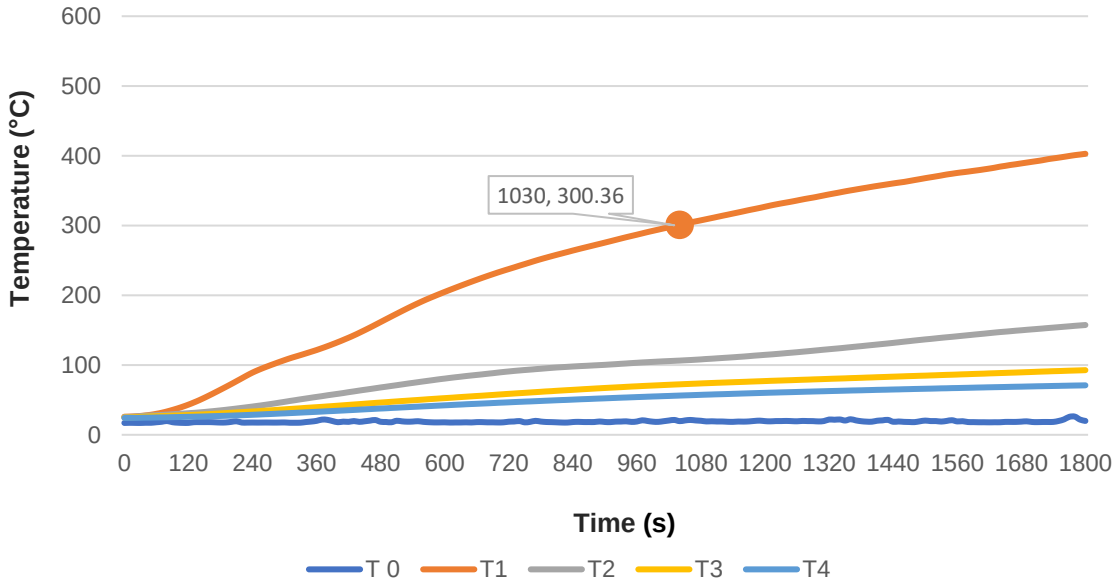

Fig. 4. Temperature profile in the sample under a thermal loading of 15 kW·m^{-2}

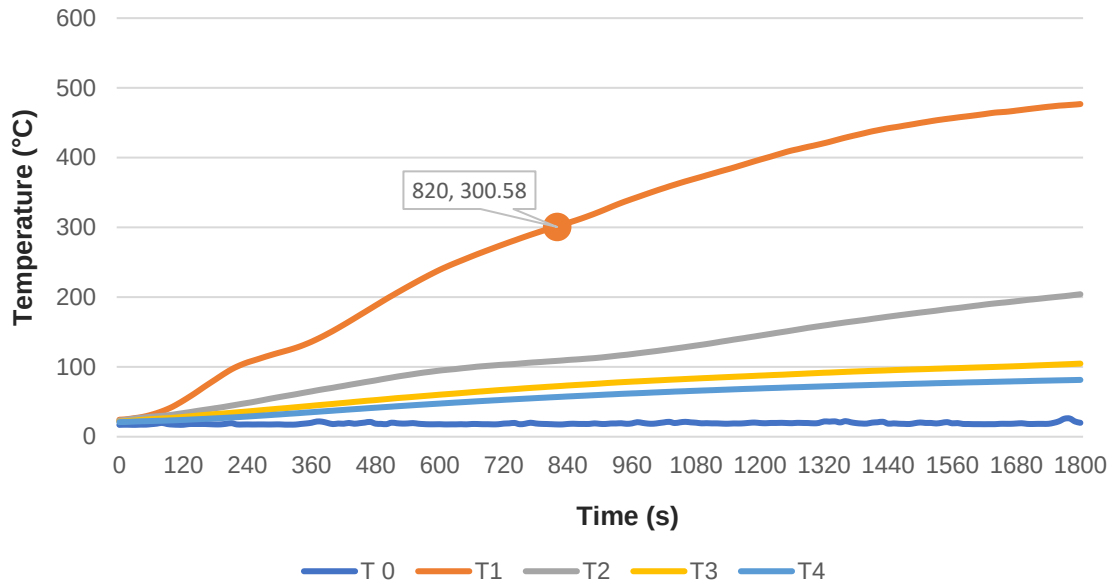

Fig. 5. Temperature profile in the sample under a thermal loading of 20 kW·m^{-2}

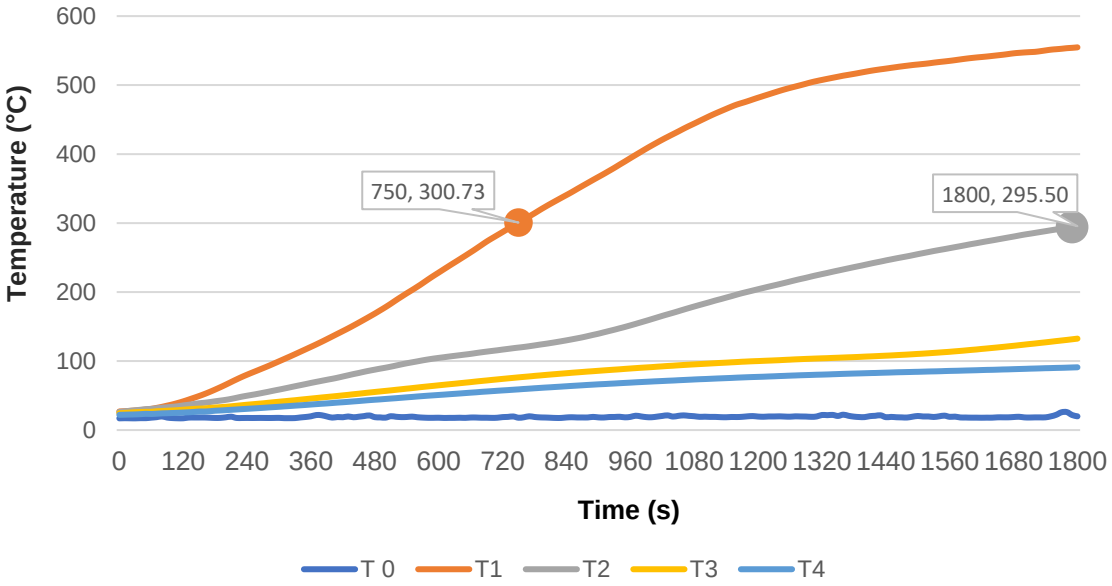

Fig. 6. Temperature profile in the sample under a thermal loading of 25 kW·m^{-2}

At a heat flux of 25 kW·m^{-2}, in a time of 1800 s, the charring temperature was not reached (a temperature of 295.50 °C was reached on thermocouple T2, which is 4.5 °C below the charring temperature). Under a thermal loading of 30 kW·m^{-2}, a temperature of 300.95 °C was reached on thermocouple T2 in a time of 1460 s, charring at the given heat flux reached a thickness of 20 mm from the thermally loaded surface. On thermocouples T3 and T4, the charring temperature of 300 °C was not reached during 1800 s, *i.e.*, at heat fluxes of 15, 20, 25 and 30 kW·m^{-2}, charring did not occur during 1800 s, at a depth of more than 20 mm from the thermally loaded surface.

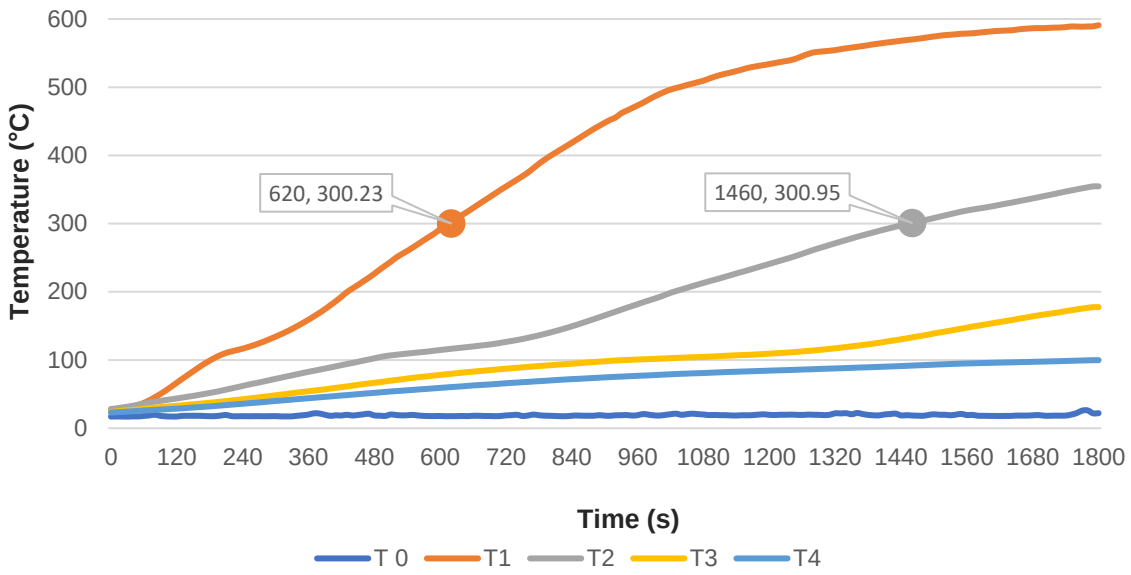

Fig. 7. Temperature profile in the sample under a thermal loading of 30 kW·m^{-2}

The above-mentioned findings are comparable to the results of studies by other authors. The temperature profile in spruce wood samples was investigated by Zachar *et al.* 2021, where a charred layer was formed at a depth up to 20 mm at heat fluxes of 15 and 20 kW·m^{-2}. According to the measurement of the temperature progression at a heat flux of 15, 20, 25 and 30 kW·m^{-2}, the charring temperature of 300 °C was not reached at a depth of 40 mm during the entire time interval.

The temperature profile and the charred layer in CLT panel sample was determined by Dúbravská *et al.* (2020). The authors found that at a distance of 200 mm from a radiation panel with dimensions of 480 x 280 mm, and at a heat flux of 43.1 kW·m^{-2}, the maximum temperature of 101.10 °C was reached at a depth of 20 mm from the thermally loaded surface, in a time interval of 30 min.

Terrei *et al.* 2020, determined the charring thickness of spruce wood samples with dimensions of 100 x 100 x 50 mm, thermally loaded using a conical calorimeter with a heat flux of 16.5 kW·m^{-2}. The charring depth of 10 mm from the thermally loaded surface was recorded in 1680 s from the beginning of the measurement. In the time up to 1800 s, a temperature of 124 °C was reached at a depth of 20 mm from the surface, *i.e.*, no charred layer was formed, which is comparable with our results. When the heat flux was increased to 35.0 kW·m^{-2}, charring was reached at a depth of 10 mm at a time of 630 s, and at a depth of 20 mm at a time of 1630 s, which is comparable with our measurements at a heat flux of 30 kW·m^{-2}.

Charring Rate

When wood is exposed to intense fire, it undergoes pyrolysis, where both a combustible gas and a char layer are formed. This char layer shields a portion of the uncharred wood from the fire intensity, thereby reducing the incident heat flux to the unburned portion on the underside of the char layer. As the char layer becomes thicker, this effect becomes increasingly significant. Therefore, if the strength of the fire's intensity is constant, the burning rate will slow and the time required for combustion will increase (Babrauskas 2004).

The charring rate of oak wood sample was calculated according to Eq. 3, *i.e.*, based on the time to reach a temperature of 300 °C and depth at which this temperature was reached. Based on measured data, average values of the charring rate were determined in the time interval from 0 to 1800 s (Tab. 1).

Table 1. Charring Rate of Samples in Time Intervals at a Depth of 10 and 20 mm

Heat Flux	Time to reach temperature 300 °C (s)		Charring Rate (mm·min^{-1})	
(kW·m^{-2})	T1	T2	β_1	β_2
15	1030	/	0.5825	/
20	820	/	0.7317	/
25	750	/	0.8013	/
30	620	1460	0.9677	0.8219

Reaching a temperature of 300 °C on thermocouple T1 was recorded at a heat flux of 15 to 30 kW·m^{-2}. At a heat flux of 15 kW·m^{-2}, the charring rate in the time interval from 0 to 1030 s was 0.582 mm·min^{-1}; at a heat flux of 20 kW·m^{-2}, the charring rate in the time interval from 0 to 820 s was 0.732 mm·min^{-1}. At a heat flux of 25 kW·m^{-2}, the average charring rate in the time interval from 0 to 750 s was 0.801 mm·min^{-1}. With a heat flux of 30 kW·m^{-2}, the average charring rate in the time interval from 0 to 620 s was 0.968 mm·min^{-1}.

Reaching a temperature of 300 °C on thermocouple T2 was recorded only at a heat flux of 30 kW·m^{-2}, calculated charring rate in the time interval from to 1460 s was 0.822 mm·min^{-1}. The relationship between the average charring rate of oak wood and the density of heat flux is shown on Fig. 8. It can be stated that the charring rate of oak wood increases with increasing heat flux, and it confirms the decreasing charring rate with increasing duration of the experiment. The reason for the decreasing charring rate is that the charred layer formed on the surface of the sample reduces the overheating and thermal decomposition of the thermally non-degraded wood under the charred layer.

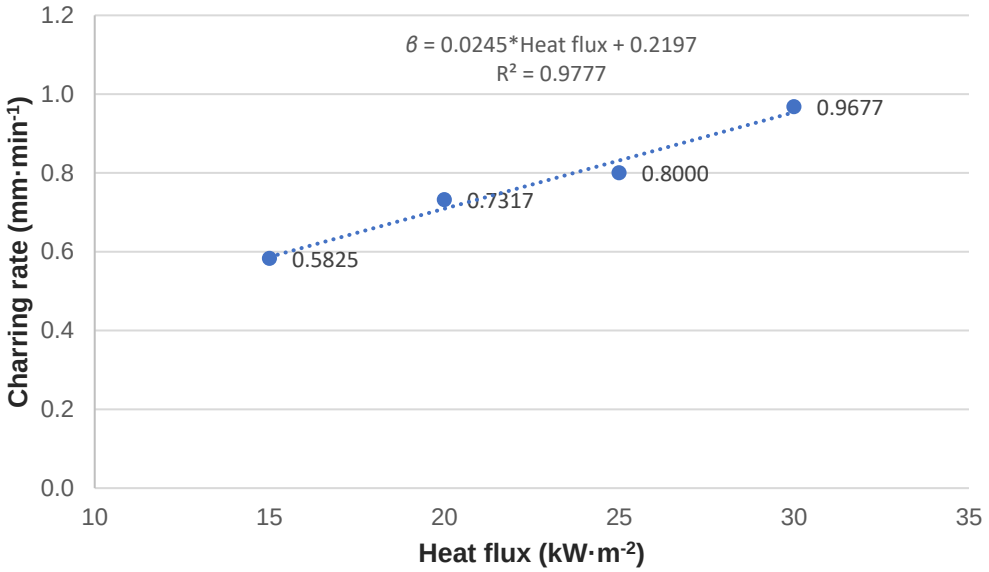

Fig. 8. Relationship between heat flux and charring rate

The charring rate is influenced not only by the heat flux, but also by the moisture content and oxygen concentration in the air (Xu *et al.* 2020). The greater the heat flux acting on the sample, the faster the charring rate, which means that in the experiment the trend was confirmed, as was expected. Zachar *et al.* (2021) also stated this claim in their experiment. When determining the charring rate of spruce wood in the time interval from 0 to 1920 s, they report the average charring rate from 1.00 mm·min^{-1} (at a heat flux of 15 kW·m^{-2}) to 1.84 mm·min^{-1} (at a heat flux of 30 kW·m^{-2}). Values of the charring rate for spruce wood were significantly higher compared to oak wood due to different wood density.

Because oak wood samples had a higher density than spruce wood, the charring rate decreased with increasing density, which corresponds to the results of scientific works of other authors (Harada 1996; Martinka *et al.* 2014; Martinka *et al.* 2018; Hao *et al.* 2020). Hao *et al.* (2020) reported values of the charring rate for oak wood in the range of 0.26 ± 0.06 mm·min^{-1} at a heat flux of 20 kW·m^{-2}, 0.58 ± 0.08 mm·min^{-1} at a heat flux of 25 kW·m^{-2}, 0.74 ± 0.09 mm·min^{-1} at a heat flux of 30 kW·m^{-2}, and 0.79 ± 0.09 mm·min^{-1} observed at a heat flux of 35 kW·m^{-2}, which is comparable to the findings reported here. Mathieu *et al.* (2023) reported in their study the charring rate of 0.35 mm·min-1 for oak wood, which is a lower rate than was determined in the present measurements.

In the conditions of real fires, in post-flashover room fires, unprotected load-bearing wooden elements will be charred at similar rate as in laboratory tests, *i.e.*, approximately 0.5 to 0.8 mm·min^{-1}. Therefore, it can be assumed that if the charring rate in a real fire does not exceed specified values, it can be useful in estimating the duration of burning time after the ignition in the room. Based on the depth of charring, *e.g.*, 30 mm, it can be estimated that at the burning rate of 0.8 mm·min^{-1}, the charring lasted at least 24 min.

Chemical Composition of Natural and Thermally Loaded Oak Wood

Increased temperature causes chemical changes in the main components of wood and extractive substances. Their range depends on the duration of the exposure and the temperature of the thermal exposure. In the temperature range of 180 to 250 °C, significant chemical changes take place in the wood. At temperatures higher than 250 °C, the charring process begins, which means that carbon dioxide and other pyrolytic products are formed (Bartlett *et al*. 2019). After the exposure to heat flux, a charred layer had been formed on the wood. Chemical analyzes were performed on the rest of oak wood samples (the charred layer was removed) after thermal stress and original wood samples (Fig. 9). The results obtained revealed that the higher value of the heat flux (over than 20, 25, and 30 kW·m^{-2}) resulted in increased extractives content in the rest of the oak wood. Comparable content of EXT was determined in samples loaded at a heat flux of 25 and 30 kW·m^{-2}, whereas these values were higher by 30% in relation to the original wood sample. Esteves *et al.* (2008) explain the increase of extractives as products of the thermal decomposition of lignin and polysaccharide macromolecules. Several authors recorded decreased content and others increased content of EXT depending on the conditions of thermal loading (*e.g.* time, temperature) (Hu *et al.* 2012; Sikora *et al.* 2018; Čabalová *et al.* 2022) and method of the EXT determination (Sharma *et al*. 2022). With a higher value of the heat flux, the content of HOLO decreased, mainly due to the lover stability of hemicelluloses compared to cellulose (Zhou *et al*. 2015; Wang *et al.* 2020). After exposure to a heat flux level of 30 kW·m^{-2}, the content of hemicellulose was lower by 10.3% compared to the original wood. A slight increase of lignin content also was observed with the higher value of the heat flux. It could have been caused by the formation of pseudo-lignin (Čabalová *et al*. 2022). During

the thermal degradation of wood, the degradation of the lignin macromolecule occurs, but also the condensation of the thermally activated lignin macromolecule with the products of the thermal degradation of polysaccharides and extractive substances (Rowel and Levan-Green 2005).

A more detailed characterization of the individual chemical components of wood is important to understand the fire safety of wood. The effect of the heat flux of 15, 20, 25 and 30 kW·m^{-2} resulted in only certain changes in the chemical composition of the rest of oak wood, primarily in the content of thermally labile hemicelluloses and in the extractives content. Lignin and cellulose are among the more stable components and ensure its strength in wood. From the point of view of changes in the chemical composition, it is likely that the rest of wood retained good strength properties even after the heat fluxes indicated.

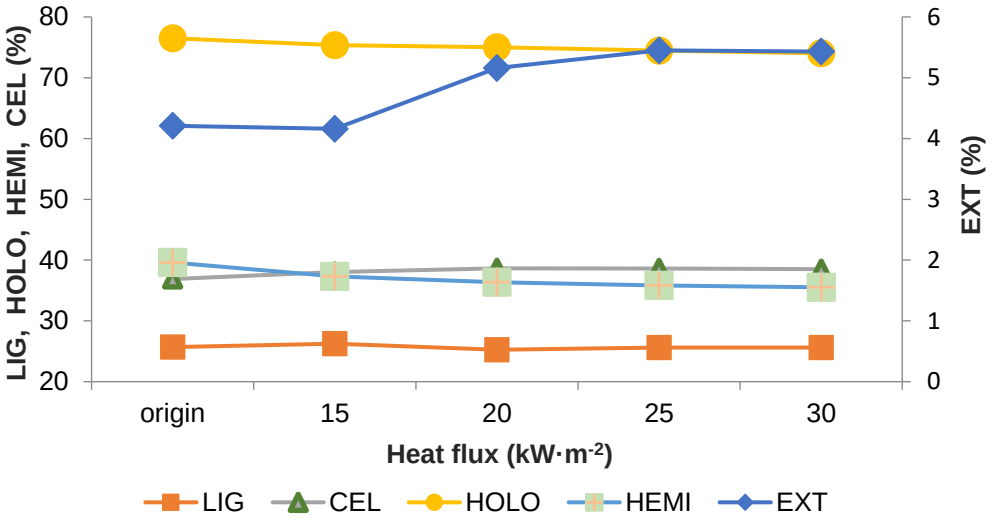

Fig. 9. Effect of heat flux on the chemical composition of oak wood; LIG – lignin, HOLO – holocellulose, HEMI – hemicelluloses, CEL – cellulose, EXT - extractives

CONCLUSIONS

1. The greater the heat flux acting on the sample, the greater the mass loss. At the lowest heat flux of 15 kW·m^{-2}, the mass loss showed the lowest values *i.e.*, 26 %, whereas at the highest heat flux of 30 kW·m^{-2}, the mass loss was almost 47 %.
2. The greater the heat flux acting on the sample, the greater the burning rate. At the lowest heat flux of 15 kW·m^{-2}, the maximum burning rate was the lowest *i.e.*, 0.0358 %·s^{-1}, whereas at the greatest heat flux of 30 kW·m^{-2}, the maximum burning rate was 0.0648 %·s^{-1}.
3. The greater the heat flux acting on the sample, the greater the charring rate. At the lowest heat flux of 15 kW·m^{-2}, the charring rate in the time interval from 0 s to 1030 s was the lowest, *i.e.*, 0.582 mm·min^{-1}. However, at the greatest charring rate of 30 kW·m^{-2}, the charring rate in the time interval from 0s to 1460 s was the greatest, *i.e.*, 0.968 mm·min^{-1}.

4. Depending on the charring rate, it is possible to estimate the fire resistance of wooden construction elements in connection with its effective cross-section in case of fire, which is detailed in the EUROCODE5 standard.
5. At a lower heat loading, the oak wood did not reach the charring temperature deeper in the sample. The charring occured only to a depth of 10 mm (thermocouple T1) at a heat flux of 15, 20, and 25 $kW \cdot m^{-2}$. The charring to the depth of 20 mm (thermocouple T2) occurred only at a heat flux of 30 $kW \cdot m^{-2}$.
6. The effect of the heat flux caused changes in the oak wood structure. A charred layer was formed, and the rest of the wood remained, on which the chemical analysis was performed. It was found that at heat flux of 30 $kW \cdot m^{-2}$, the amount of extractive substances in the sample increased by 30% and thermally labile hemicelluloses decreased by 10.3% compared to the original samples. The content of thermally more stable both lignin and cellulose did not change. It is therefore possible to conclude that, from the point of view of the chemical composition, no significant changes occurred in the rest of the wood.

ACKNOWLEDGMENTS

This work was supported by the Scientific Grant Agency of the Ministry of Education, Research, Development and Youth of the Slovak Republic and the Slovak Academy of Sciences under the Contract VEGA no. 1/0115/22 A comprehensive approach to the study of changes in fire parameters using progressive analytical and testing methods.

This work was supported by the Slovak Research and Development Agency under the Contract no. APVV-22-0030.

REFERENCES CITED

ASTM D1107-21 (2021). "Standard test method for ethanol-toluene solubility of wood," ASTM International, West Conshohocken, PA, USA.

Babrauskas, V. (2004). "Wood char depth interpretation in fire investigations," in: *Proceedings of the 10th International Fire Science and Engineering (Interflam) Conference*, Interscience Communications, Ltd., London.

Babrauskas, V. (2005). "Charring rate of wood as a tool for fire investigations," *Fire Safety Journal* 40, 528-554. DOI: 10.1016/j.firesaf.2005.05.006

Bartlett, A. I., Hadden, R. M., and Bisby, L. A. (2019). "A review of factors affecting the burning behaviour of wood for application to tall timber construction," *Fire Technology* 55, 1-49. DOI: 10.1007/s10694-018-0787-y

Booth, H. (1987). *Carbonisation Processes. How Wood is Transformed into Charcoal*, The FAO Technical Papers. ISBN 92-5-101328-1

Čabalová, I., Výbohová, E., Igaz, R., Krišťák, L., Kačík, F., Antov, P., and Papadopoulos, A. N. (2022). "Effect of oxidizing thermal modification on the chemical properties and thermal conductivity of Norway spruce (*Picea abies* L.) wood," *Wood Material Science Eng.* 17, 366-375.

Cachim, P. B., and Franssen, J. F. (2008). "Comparison between the charring rate model and the conductive model of Eurocode 5," *Fire and Materials* 33(3), 129-143. DOI: 10.1002/fam.985

Chen, T., Wu, W., Wu, J., Cai, J., and Wu, J. (2016). "Determination of the pseudo components and kinetic analysis of selected combustible solid wastes pyrolysis based on Weibull model," *J. Therm. Anal. Calorim.* 126, 1899-1909. DOI: 10.1007/s10973-016-5649-6

Dúbravská, K., Tereňová, Ľ., and Štefková, J. (2020). "CLT construction performance under thermal loading," *Wood Research* 65(4), 605-614. DOI:10.37763/wr.1336-4561/65.4.605614

Findorák, R., Fröhlichová, M., Legemza, J., Findorákova, L. (2016). "Thermal degradation and kinetic study of sawdusts and walnut shells via thermal analysis," *J. Therm. Anal. Calorim*125, 689-694. DOI: 10.1007/s10973-016-5264-6

Friquin, K. L. (2011). "Material properties and external factors influencing the charring rate of solid wood and glue-laminated timber," *Fire and Materials* 35, 5, 303-327. DOI: 10.1002/fam.1055

Hao, H., Chow, Ch. L., and Lau, D. (2020). "Effect of heat flux on combustion of different wood species," *Fuel* 278, 118325. DOI: 10.1016/j.fuel.2020.118325

Harada, T. (1996). "Charring of wood with thermal radiation. II. Charring rate calculated from mass loss rate," *Mokuzai Gakkaishi* 42, 194-201.

Hasburgh, R. H., and Dietenberger M. A. (2001). *Wood Products: Thermal Degradation and Fire*, U.S. Department of Agriculture, Forest Products Laboratory, Madison, WI, USA. DOI: 10.1016/B978-0-12-803581-8.03338-5

Hrovatin, J. (2005)." Contemporary systems of prefabricated wooden house construction," *Wood in the Construction Industry: Durability and Quality of Wooden Construction Products. Proceedings Paper*, pp. 21-26. ISBN 953-6307-80-4

Hu, C., Jiang, G., Xiao, M., Zhou, J, and Li, Z. (2012). "Effects of heat treatment on water-soluble extractives and colour changes of merbau heartwood," *Journal Wood Science* 58, 465-469. DOI: 10.1007/s10086-012-1265-7

ISO 10694 (1995). "Soil quality. Determination of organic and total carbon after dry combustion (elementary analysis)," International Organization for Standardization: Geneva, Switzerland.

ISO 11885 (2007). "Water quality. Determination of selected elements by inductively coupled plasma optical emission spectrometry (ICP-OES)," International Organization for Standardization, Geneva, Switzerland.

ISO 13878 (1998). "Soil quality. Determination of total nitrogen content by dry combustion (elemental analysis)," International Organization for Standardization, Geneva, Switzerland.

ISO 13927 (2015). "Plastics — Simple heat release test using a conical radiant heater and a thermopile detector," International Organization for Standardization: Geneva, Switzerland.

ISO 15178 (2000). "Soil quality. Determination of total sulphur by dry combustion," International Organization for Standardization, Geneva, Switzerland.

ISO 17554. (2014). "Reaction to fire tests — Mass loss measurement," International Organization for Standardization: Geneva, Switzerland.

Kačíková, D., and Makovická-Osvaldová, L. (2009). "Wood burning rate of various three parts from selected woods," *Acta Fac. Xylologiae Zvolen* 2009, 27-32.

Kačíková, D., Majlingová, A., Veľková, V., and Zachar, M. (2017). *Modelling of Internal Fires Using the Results of Progressive Methods of Fire Engineering* (1st ed.), Technical University, Zvolen, Slovakia.

Kamenická, Z., Sandanus, J., Blesák, L., Cábová, K., and Waldt, F. (2018). "Methods for determining the charring rate of timber and their mutual comparison," *Wood Research* 63(4), 583-590.

Kim, M., Kim, S., Kim, C., and Shim, K. (2022). "Determination of charring thickness of wood by residual strength analysis," *BioResources* 17(1), 1485-1493. DOI: 10.15376/biores.17.1.1485-1493

Kmeťová, E., Kačík, F., Kubovský, I., and Kačíková, D. (2022). "Effect of expandable graphite flakes on the flame resistance of oak wood," *Coatings* 12 (12), article ID1908. DOI: 10.3390/coatings12121908

Kravetz, C., Leca, C., Brito, J. O., Saloni, D., and Tilotta, D. C. (2020). "Characterization of selected pyrolysis products of diseased orange wood," *BioResources* 15(3), 7118-7126. DOI: 10.15376/biores.15.3.7118-7126

Liu, C., Deng, Y., Ws, S., Lei, M., and Liang, J. (2016). "Experimental and theoretical analysis of the pyrolysis mechanism of a dimeric lignin model compound with α-O-4 linkage," *BioResources* 11(2), 3626-3636. DOI: 10.15376/biores.11.2.3626-3636

Lowden, L. A., and Hull, T. R. (2013). "Flammability behaviour of wood and a review of the methods for its reduction," *Fire Science Review* 2. DOI: 10.1186/2193-0414-2-4

Martinka, J., Hroncová, E., Chrebet, T., and Balog, K. (2014). "The influence of spruce wood heat treatment on its thermal stability and burning process," *European Journal of Wood and Wood Products* 72, 477-486. DOI: 10.1007/s00107-014-0805-9

Martinka, J., Rantuch, P., and Loner, M. (2018). "Calculation of charring rate and char depth of spruce and pine wood from mass loss," *Journal of Thermal Analysis and Calorimetry* 132, 1105-1113. DOI: 10.1007/s10973-018-7039-8

Mathieu, S., Erez, G., Chaouchi, M., Bretonnet, Ch., and Thiry, A. (2023). "Relationship between char depth of wood and cumulative heat exposure for fire investigation," *Fire Safety Journal* 140, article 103856. DOI: 10.1016/j.firesaf.2023.103856

Mensah, R. A, Jiang, L., Renner, S. J., and Xu, Q. (2023). "Characterisation of the fire behaviour of wood: From pyrolysis to fire retardant mechanisms," *Journal of Thermal Analysis and Calorimetry* 24, 1-16. DOI: 10.1007/s10973-022-11442-0

Mikkola, E. (1991). "Charring of wood based materials," *Fire Safety Science* 3, 547-556. DOI: 10.3801/IAFSS.FSS.3-547

NFPA 921 (2021). "Guide for fire and explosion investigations," National Fire Protection Association, Quincy, MA, USA.

Njankouo, J. M., Dotreppe, J. C., and Franssen, J. M. (2004). "Experimental study of the charring rate of tropical hardwoods," *Fire and Materials* 28, 15. DOI: 10.1002/fam.831

Osvald, A. (2010). *Drevostavba ≠ Požiar*, Technical University of Zvolen, Zvolen, Slovakia.

Poletto, M., Zattera, A. J., and Santana, R. M. C. (2015). "Structural differences between wood species: Evidence from chemical composition, FTIR spectroscopy, and thermogravimetric analysis," *Journal of Applied Polymer Science* 126, 337-344. DOI: 10.1002/app.36991

Protić, M., Mišić, N., Raos, M., and Sekulić, S. (2020). "Solid wood flammability testing," *Safety Engineering* 10(1), 9-12. DOI: 10.5937/SE2001009P

Qin, R., Zhou, A., Chow, C. L., and Lau, D. (2021). "Structural performance and

charring of loaded wood under fire," *Eng. Struct.* 228, article 111491. DOI: 10.1016/j.engstruct.2020.111491

Reinprecht, L. (1997). *Procesy Degradácie Dreva*, Technical University of Zvolen, Zvolen, Slovakia.

Richter, F., Atreya, A., Kotsovinos, P., and Rein, G. (2019). "The effect of chemical composition on the charring of wood across scales," *Proc. Combust. Inst.* 37, 4053-4061. DOI: 10.1016/j.proci.2018.06.080

Rowel, R. M., and Levan-Green, S. L. (2005). "Thermal properties," in: *Handbook of Wood Chemistry and Wood Composites*, R. M. Powell (ed.), CRC Press, Boca Raton, FL, USA.

Salmen, L., Olsson, A. M., Stevanic, J. S., Simonovic, J., and Radotic, K. (2011). "Structural organisation of the wood polymers in the wood fibre structure," *Proceedings Paper*, 7-12. ISBN 978-7-5019-8206-6

Seifert, V. K. (1956). "About a new method for rapid determination of pure cellulose (in German)," *Das Papier*10, 301-306.

Sharma, V., Kumar, R., Dutt, B., and Attri, V. "Influence of heat treatment on chemical and mechanical properties of *Toona ciliata* M. Roem," *Wood. Mat. Sci. Res. India* 19, 1. DOI: 10.13005/msri/190105

Sikora, A., Kačík, F., Gaff, M., Vondrová, V., Bubeníková, T., and Kubovský, I. (2018). "Impact of thermal modification on color and chemical changes of spruce and oak wood," *Journal Wood Science* 64, 406-416. DOI: 10.1007/s10086-018-1721-0

Sluiter, A., Hames, B., Ruiz, R., Scarlata, C., Sluiter, J., Templeton, D., and Crocker, D. (2012). *Determination of Structural Carbohydrates and Lignin in Biomass (NREL/TP-510-42618)*, National Renewable Energy Laboratory, Golden, CO.

Špilák, D., Tereňová, L., Dúbravská, K., and Majlingova, A. (2018). "Analysis of carbonized layer of wood beams with different geometric cross-section shape," *Delta* 12(2), 65-81. DOI: 10.17423/delta.2018.12.2.53

Terrei, L., Acem, Z., Marchetti, V., Lardet, P., Boulet, P., and Parent, G. (2021) "In-depth wood temperature measurement using embedded thin wire thermocouples in cone calorimeter tests," *International Journal of Thermal Sciences* 162, article 106686. DOI: 10.1016/j.ijthermalsci.2020.106686

UMN no. 9373, PUV 50121-2020. "Method of determination and apparatus for determination of burn-off rate and the carbonization rate of polymers using the flame initiator," IPO WebRegisters - UV 50121-2020 (gov.sk)

Wang, J., Minami, E., and Kawamoto, H. (2020). "Thermal reactivity of hemicellulose and cellulose in cedar and beech wood cell walls," *Journal Wood Science* 66, 41. DOI: 10.1186/s10086-020-01888-x

White, R. H., and Nordheim, E. V. (1992). "Charring rate of wood for ASTM E 119 exposure," *Fire Technol.* 28, 5-30. DOI: 10.1007/BF01858049

Wise, L. E., Murphy, M., and D'Addieco, A. A. (1946). "Chlorite holocellulose, its fractionation and bearing on summative wood analysis and on studies on the hemicelluloses," *Paper Trade Journal* 122, 35-44.

Xu, M., Tu, L., Cui, Z., and Chen, Z. (2020). "Charring properties and temperature profiles of laminated bamboo under single side of ISO 834 fire exposure," *BioResources* 15(1), 1445-1462. DOI: 10.15376 /biores.15.1.1445-1462

Zachar, M., Čabalová, I., Kačíková, D., and Zacharová, L. (2021). "The effect of heat flux to the fire-technical and chemical properties of spruce wood (*Picea abies* L.)," *Materials (Basel)*14, article 4989. DOI: 10.3390/ma14174989

Zanatta, P., Peres, M. L., Gallio, E., Ribes, D. D., Lazarotto, M., Gatto, D. A., and Moreira, M. L. (2018)." Reduction of flammability of *Pinus elliottii* wood modified with TiO_2 particles," *Matéria (Rio de Janeiro)* 23(1), article 481. DOI: 10.1590/S1517-707620180001.0481

Zhou, A., Qin, R., Chow, C. L., and Lau, D. (2020). "Bond integrity of aramid, basalt and carbon fiber reinforced polymer bonded wood composites at elevated temperature," *Compos. Struct*. 245, article 112342. DOI: 10.1016/j.compstruct.2020.112342

Zhou, H., Long, Y., Meng, A., Chen, S., Li, Q., and Zhang, Y. (2015). "A novel method for kinetics analysis of pyrolysis of hemicellulose, cellulose, and lignin in TGA and macro-TGA," *RSC Adv.* 5, 26509-26516. DOI: 10.1039/C5RA02715B

Article submitted: June 20, 2024; Peer review completed: August 18, 2024; Revised version received: November 6, 2024; Accepted: November 7, 2024; Published: November 26, 2024.
DOI: 10.15376/biores.20.1.860-876